

Channel-to-Rib Width Ratio Effects of Flowfield Plates in the Performance of a Micro-PEM Fuel Cell Stack

Bing-Shyan Her, Shou-Shing Hsieh,* and Jyun-Hong Chen

Department of Mechanical and Electro-Mechanical Engineering, National Sun Yat-Sen University,
Kaohsiung, Taiwan 80424, ROC

*Email : sshsieh@faculty.nsysu.edu.tw

ABSTRACT

Effect of channel-to-rib width ratio of flow channel plates on micro proton exchange membrane fuel cell stacks performance test (VI/PI) was studied experimentally. The channel-to-rib width ratio was varied from 0.5 to 2. The optimum channel-to-rib width ratio of flow channel plates for micro PEM fuel cell stack was found. Copper metals were used to make bipolar plates (BPs) by using a LIGA-like micro-fabrication process of deep UV lithography in order to obtain SU-8 resist patterns/and SU-8 mould. Moreover, when the VI/PI performance curves were considered, an optimum channel-to-rib width ratio of 1 can be also obtained for the present study.

Keywords: channel-to-rib width ratio, micro-PEM fuel cell

1 INTRODUCTION

Proton exchange membrane (PEM) fuel cell stack has many advantages compared with other types of fuel cell stacks as portable power for mobility [1]. The application of fuel cell stacks to portable power is motivated by numerous occasions such as 3C products [2]. This is because the PEM fuel cell stack presents a high power density and operates at a relatively low temperature; two qualities which make it ideal for portable systems [3]. Further, the use of micro-fabrication technology for fulfillment of power generation has ever been increased with being widely and generally demanded in portable electronic applications especially for 3C products [3-5]. One of the notable and promising examples is micro-fuel cell stack system, for instance, micro-PEM fuel cell stack/micro-direct methanol (DM) fuel cell stack, which is now target for battery replacement for portable electronic devices and miniature power source [5]. The micro-fuel cell stacks are expected to attain higher energy density than that of a lithium ion battery by converting hydrocarbon fuel to electric power at several percentage or higher efficiency. A micro fuel cell stack power source can be considered as an approach that combines thin film materials with micro-electromechanical system (MEMS) technology [6]. Generally, fuel cell stacks performance would increase in gas velocity would facilitate reactant delivery to reaction sites by improved convective mass transport in a narrower flow channels.

It is known that the flow channel design influences not only the stack resistance but the mass transport of reactant gases and liquids. For a conventional PEM fuel cell stacks, the main goals of flow channel design are to increase the uniformity of the current and temperature distribution at the operating conditions of interest while keeping or improving the stack performance [4]. Studies of different flow patterns will give a concept of how to optimize the flow channel design for a PEM fuel cell stack. This optimization would be obviously changed with the stack operating conditions.

Data have shown that quick gas diffusion favors wider channel (narrower rib) width of flow channels. However, for a higher electric conduction, a narrower channel (i.e. wider rib) of flow channel configuration is needed to achieve a higher electric conduction. Therefore, it is necessary to investigate the geometric parameters involved with flow channels such as the flow channel type, the channel-to-rib width ratio, the rib shape, and the diffusion layer thickness on cell performance and pressure drop in detail as well.

Although there are a plenty of papers dealt with PEM fuel cells, few papers have reported works on a micro-fuel cell stack flow configuration especially with an optimum channel-to-rib width ratio. Further, there seems to be that no open literature available to discuss the effect for both the cell stack performance and flow channel pressure drop simultaneously. In this work, effects of channel-to-rib width (with a rectangular cross-section) ratio of the serpentine flow channel on cell stack performance and pressure drop will be studied. An optimum operating condition with a trade-off to channel-to-rib width ratio will be obtained.

In this study, we will focus on three different 5 cm² flow channel patterns with various rib widths and a given channel size for 28-channel serpentine, 36-channel serpentine, and 44-channel serpentine flows as listed in Table 1. Basically, they have similar patterns with three different gas path lengths. They were so designed that the effects of flow pattern and the path length on the cell stack performance and pressure drop can be examined simultaneously to provide and develop the generic design information for flow channels, which might be beneficial to the fuel cell stack industry especially for micro-fuel cell stack manufacturers. This present study is a part of our main research goal of design and fabrication of a high performance micro-PEM fuel cell stack.

Case	1	2	3
Channel width (μm)	300	300	300
Rib width (μm)	600	300	150
Channel length (mm)	160	205	250
Channel pass	4	5	6
Channel number	28	36	44
Channel-to-rib width ratio	0.5	1.0	2.0
Open ratio (%)	37.9	49.2	60.0
Channel depth (μm)	200		
Reynolds number (anode)	6.26		
Reynolds number (cathode)	229.03		
Knudsen number (anode)	4.97×10^{-4}		
Knudsen number (cathode)	2.60×10^{-4}		
Mach number (anode)	0.0021		
Mach number (cathode)	0.0402		

Table 1 Geometry of bipolar plates

Copper metals were used to make bipolar plates (BPs) by using a LIGA-like micro-fabrication process of deep UV lithography in order to obtain SU-8 mould. The bipolar plate has many flow channels on each side that are designed for supplying fuel and oxidant. They are designed to accomplish the following functions : (a) distribute reactants uniformly over the active areas ; (b) remove heat from the active areas ; (c) act as current collector ; (d) keep reactants separate ; and (e) prevent leakage of reactants. In addition, the plates should not only be of inexpensive, high electric (ion) and thermal conductivity materials, and also easily manufactured. Efforts are now underway to develop BP materials that satisfy the aforementioned demands. Among those possible BP materials, copper (Cu) has high mechanical strength and stability, electric conductivity and thermal conductivity and can be easily fabricated to the desired shape to accommodate the flow channels. However, due to its weight, copper is infrequently considered as a BP material.

2 EXPERIMENTAL

2.1 Bipolar plates preparation

Copper slims (250 μm thick) were used as substrates (base plates). An electrolytic direct current (dc) plating process was used in the subsequent stage after defining the SU-8 mould for the fabrication of Cu bipolar plates with serpentine (meandering) flow channels. Detailed fabrication steps in sequence and fabrication parameters and operating conditions are shown in Table 2. Then, the substrate was first cleaned with acetone for 3 min and then heated to 150 $^{\circ}\text{C}$ for another 3 min for dryness. After the substrate cooled

down enough to reach ambient temperature, SU-8 (2100) (MicroChem, Newton, MA) was spun-coated on the Cu substrate with a final thickness of 200 μm . The spin speed starts at zero with a linear increase to 400 rpm (slop : 100 rpm/s) for 4 s followed by a constant speed for 36 s. Then, the spin speed increases again linearly with the same slop as previously for 3 s. Finally, the speed is maintained at 700 rpm for 57 s. The total spinning time is 100 s.

The SU-8 coated Cu film in the soft baking process was heated on a hotplate, based on the following steps : first it was baked at 65 $^{\circ}\text{C}$ for 5 min, then at 95 $^{\circ}\text{C}$ for another 70 min. To avoid the shrinkage and wrinkling of SU-8 and Cu substrates, it was firstly cooled to 65 $^{\circ}\text{C}$ for 5 min. Then, the relaxed SU-8 and Cu substrate was kept at room temperature on a flat plate for 50 min. After soft baking, a pre-designed (by CAD software) and prepared by a 10,000 dpi (photo-resist width $\geq 15 \mu\text{m}$) image setter photo-mask was aligned in position. Then, SU-8 and Cu substrate was exposed to UV light (Hg lamp with wavelength of 365 nm, 33mW/cm²) for 75 s using a UV aligner. Meanwhile, SU-8 was simultaneously lithographically structured. Once exposure was completed, heat was applied again for post-baking. It was first heated to 65 $^{\circ}\text{C}$ for 2 min, followed by 17 min heating at 95 $^{\circ}\text{C}$ on a hotplate. Similarly, it was cooled to 65 $^{\circ}\text{C}$ for 5 min and then relaxed at room temperature. Using Nano SU-8 developer (MicroChem, Newton, MA), the development was done with an ultrasonic wave oscillator for 3 min.

Before performing electroplating, the rinsing of SU-8 patterned structure in acetone had to be properly controlled and applied for at least 1 min. Then, it was completely and carefully rinsed again in de-ionized (DI) water. The patterned SU-8 channel structure (200 μm depth, 300 μm width and different rib width) was electroformed with copper using copper sulfate and H₂SO₄ solution with dc applied at a current density 20 mA/cm². The pH 4 and 31.6 $^{\circ}\text{C}$, respectively, to avoid damage of the plated surface by hydrogen bubbles. In fact, quite a few bubbles are generated due to good agitation, and the bubbles are quite small ; they cannot be observed by the naked eye. After plating, the Cu microstructure was obtained when the SU-8 mould was stripped off by remover propylene glycol remover (PG, MicroChem, Newton, MA) and rinsed by DI water in an ultrasonic wave oscillator at 70 $^{\circ}\text{C}$ for 20 min. The most suitable operating condition was at the above-stated temperature and time duration with 40% ultrasonic wave oscillation assistance. Since PG remover is acidic by nature, a time reduction for water bath would assist in securing a more uniform and flat surface. Deteriorating adhesion of the copper structure to the substrate apparently never occurred.

Now, the Cu end plate had been obtained. For a bipolar plate, we needed to go through the processes again after flipping over the substrate. The present micro-fabrication and products characterization were done at MEMS Laboratory of National Taiwan Normal University and

Fabrication parameters and conditions		
PR coating	SU-8 2100	
PR property	Negative	
PR type	Thick film	
Dehydration bake (°C)	150	
Speed (rpm)	450 (40sec) ; 950 (60sec)	
Soft bake (95 °C) (min)	150	
UV light wave length (nm)	365	
Light intensity (mW/cm ²)	17	
Exposure time (s)	50	
Post exposure bake (95 oC) (min)	30	
Development (min)	3	
Electroforming solution	Copper sulfate, H ₂ SO ₄ solution	
Solution pH	4	
Solution temperature (°C)	50	
Current density (mA/cm ²)	10	
Photoresist remover	Remover propylene glycol	
Experiment operating parameters		
Inlet gas	Anode	Hydrogen (99.99%)
	Cathode	Air
Flow rate	Anode	20 sccm 30 sccm
	Cathode	100 sccm 150 sccm
Gas backpressure	Anode	97 kPa
	Cathode	97 kPa
MEAs	Nafion 117	Anode: Pt on carbon (0.5 mg/cm ²)
		Cathode: Pt on carbon (0.5 mg/cm ²)
	GDL	Anode: Carbon paper based material (290 m)
		Cathode: Carbon paper based material (290 m)
Electrode	Copper	
Active area	5 cm ²	
Cell number	2 cell stack and 3 cell stack	

Table 2 Fabrication parameters and conditions/experiment operating parameters

2.2 Stack H₂/Air circulating loop and experimental conditions

The computer controlled micro-PEM fuel cell stacks system and circulating loop is designed (see Fig. 1 for details) for operation with hydrogen and air. The reactant

gases are fed in series to the stacks. Hydrogen (H₂) and air are conducted parallel-flow mode by varying channel/pass (serpentine) as also listed in Table 1 on both the anode and cathode of the stacks. Purified (99.99%) and dry hydrogen is fed into the cell form a gas cylinder through a mass flow meter and back-pressure valve and compressed air was provided. Current density versus voltage curves of the stack were taken using a KIKUSUI PLZ16WA system interfaced to a personal computer (PC) at constant current and recorded after the system reached a stable steady state (about 1 h) under the different operating conditions at a reasonable current density. The fuel cell system used was similar to that of Hsieh et al [4]. The stand includes a electro-loading system (KIKUSUI PLZ16WA) for fuel cell stack operation and data acquisition for generation of a polarization curve (both VI and PI curve) to compare performance. Test with respect to performance and lifetime of the cell stack are in progress. The cell stack was operated at 25 °C.

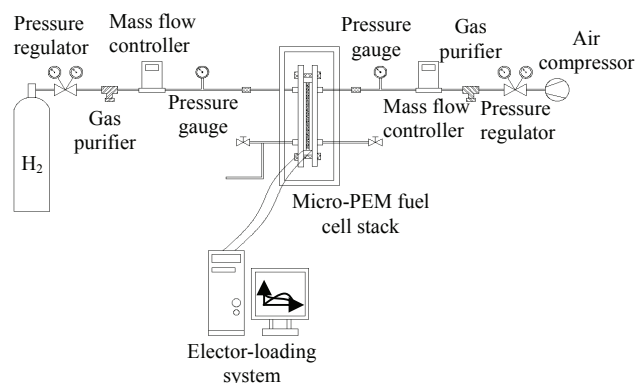


Fig. 1 Schematic of experimental apparatus for the present cell stacks

3 RESULTS AND DISCUSSION

3.1 Channel-to-rib width ratio on VI/PI curves

Fig. 2 exhibits a performance test expressed by VI/PI curves with 2 cell stacks and fixed operating temperature of 25 °C and same operating pressure $P_{\text{anode}} = P_{\text{cathode}} = 97 \text{ kPa}$ in different channel-to-rib width ratio (0.5, 1, and 2). As expected, the open circuit voltage (OCV) 1.89 V, 2.03 V, and 1.97 V/limiting current density 486.6 mA/cm², 523.2 mA/cm², and 507.5 mA/cm², in different channel-to-rib width ratio 0.5, 1, and 2, respectively. Fig. 3 presents a performance test expressed by VI/PI curves with 3 cell stacks and fixed operating temperature of 25 °C and same operating pressure $P_{\text{anode}} = P_{\text{cathode}} = 97 \text{ kPa}$ in different channel-to-rib width ratio (0.5, 1, and 2). As expected, the open circuit voltage (OCV) 2.70 V, 2.90 V, and 2.81 V/limiting current density 493.2 mA/cm², 530.3 mA/cm², and 514.4 mA/cm², in different channel-to-rib width ratio

0.5, 1, and 2, respectively. In order to enhance and broaden our fundamental understanding, stack OCV as well as stack average power density were plotted against the channel-to-rib width ratio, and different cell stack number, respectively, at $T_{\text{stack}} = 25\text{ }^{\circ}\text{C}$, $P_{\text{anode}} = P_{\text{cathode}} = 97\text{ kPa}$, and the results are thus shown in Fig. 4.

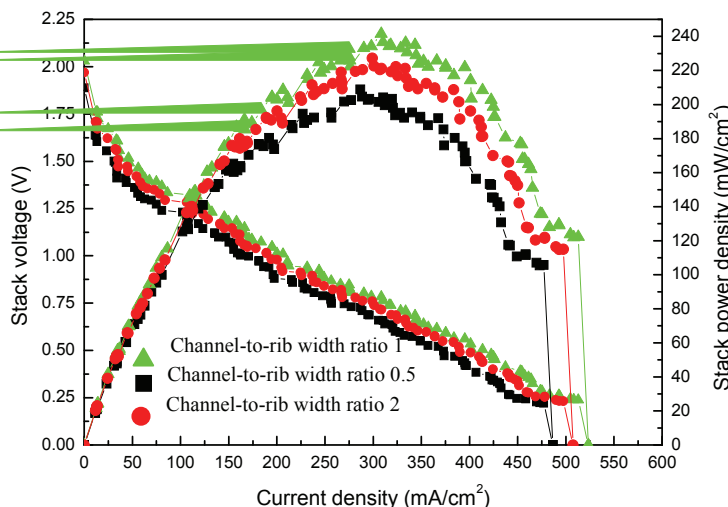


Fig. 2 The performance test for 2 cell stacks with an optimum condition

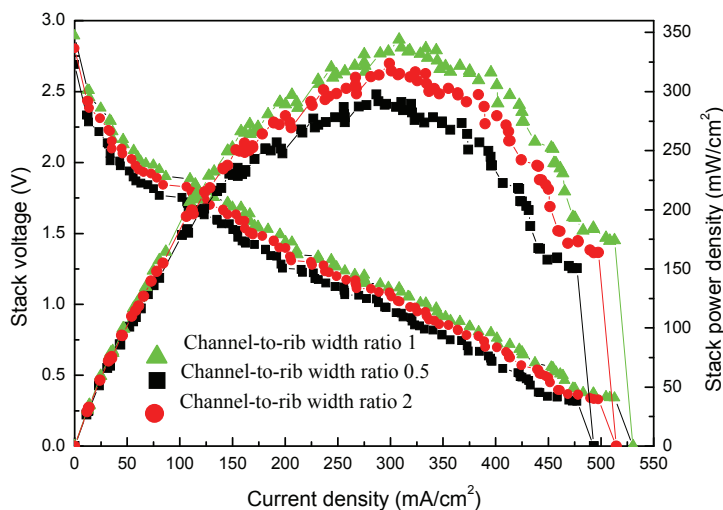


Fig. 3 The performance test for 3 cell stacks with an optimum condition

It is known that the dimensions of the channels and their spacing affect the reactant gas (H_2/Air) access to the gas diffusion layer and also provide wide area for water removal from the gas diffusion layer. This would result in an increase in proton conductivity. However, this could also cause a poor electron transfer due to a narrow spacing. On the contrary, wide spacing enhances conduction of electrical current and heat ; however, it simultaneously reduces the area directly exposed to the reactants and promotes the accumulation of water. Consequently, it results in a poor stack performance. In fact, it was found to be 1 in the present study.

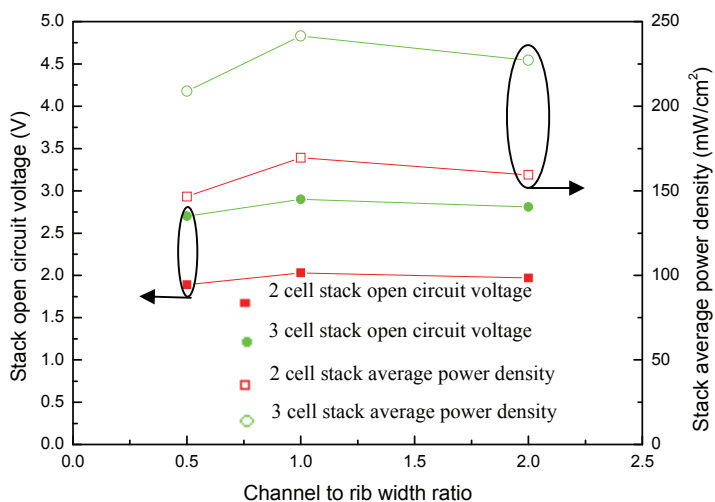


Fig. 4 The stack open circuit voltage and the stack average power density vs. channel-to-rib width ratio

4 CONCLUSIONS

The channel and rib geometric scale effects of flow channel plates/bipolar plates on the performance of micro-PEM fuel cell stacks were examined and discussed. Only VI/PI performance curves considered, the above-stated value would become a little bit bigger, an optimum channel-to-rib width ratio in the range of the present study of 0.5-2 was found to be 1.

REFERENCES

- [1] C.-Y. Chen, W.-H. Lai, B.-J. Weng, H.-J. Chuang, C.-Y. Hsieh, and C.-C. Kung, "Planar Array Stack Design Aided by Rapid Prototyping in Development of Air-Breathing PEMFC," *Journal of Power Sources*, Vol. 179, pp. 147-154, 2008.
- [2] G. Scrivano, A. Piacentino, and F. Cardona, "Experimental Characterization of PEM Fuel Cell by Micro-Models for the Prediction of On-Site Performance," *Renewable Energy*, Vol. 34, pp. 634-639, 2009.
- [3] S.-S. Hsieh, C.-L. Feng, and C.-F. Huang, "Development and Performance Analysis of a H_2/air Micro PEM Fuel Cell Stack," *Journal of Power Sources*, Vol. 163, pp. 440-449, 2006.
- [4] S.-S. Hsieh, and K.-M. Chu, "Channel and Rib Geometric Scale Effects of Flowfield Plates on the Performance and Transient Thermal Behavior of a Micro-PEM Fuel Cell," *Journal of Power Sources*, Vol. 173, pp. 222-232, 2007.
- [5] S.-S. Hsieh, C.-F. Huang, and C.-L. Feng, "A Novel Design and Micro-Fabrication for Copper (Cu) Electroforming Bipolar Plates," *Micron*, Vol. 39, pp. 263-268, 2008.
- [6] P.-C. Lin, B. Y. Park, and M. J. Madou, "Development and Characterization of a Miniature PEM Fuel Cell Stack with Carbon Bipolar Plates," *Journal of Power Sources*, Vol. 176, pp. 207-214, 2008.